Available online at www.sciencedirect.com
ScienceDirect
Bioorganic Chemistry 35 (2007) 175–188
BIOORGANIC CHEMISTRY
www.elsevier.com/locate/bioorg

# Iron- and 4-hydroxy-2-alkylquinoline-containing periplasmic inclusion bodies of *Pseudomonas aeruginosa*: A chemical analysis

Paulette W. Royt [a,*], Robert V. Honeychuck [b], Ramesh R. Pant [b], Magnus L. Rogers [b], Ludmila V. Asher [c], John R. Lloyd [d], W.E. Carlos [e], Harvey E. Belkin [f], Swati Patwardhan [a]

[a] *Molecular and Microbiology Department, George Mason University, Fairfax, VA 22030, USA*
[b] *Chemistry and Biochemistry Department, George Mason University, Fairfax, VA 22030, USA*
[c] *Division of Pathology, Walter Reed Army Institute of Research, Silver Spring, MD 20910, USA*
[d] *NIDDK, NIH, DHHS, Bethesda, MD 20892, USA*
[e] *Naval Research Laboratory, Washington, DC 20375, USA*
[f] *U.S. Geological Survey, Reston, VA 20192, USA*

Received 7 September 2006
Available online 28 November 2006

**Abstract**

Dark aggregated particles were seen on pellets of iron-rich, mid-logarithmic phase *Pseudomonas aeruginosa*. Transmission electron microscopy of these cells showed inclusion bodies in periplasmic vacuoles. Aggregated particles isolated from the spent medium of these cells contained iron as indicated by atomic absorption spectroscopy and by electron paramagnetic resonance spectroscopy that revealed $Fe^{3+}$. Scanning electron microscopy/energy dispersive X-ray analysis of whole cells revealed the presence of iron-containing particles beneath the surface of the cell, indicating that the isolated aggregates were the intracellular inclusion bodies. Collectively, mass spectroscopy and nuclear magnetic resonance spectroscopy of the isolated inclusion bodies revealed the presence of 3,4-dihydroxy-2-heptylquinoline which is the *Pseudomonas* quinolone signaling compound (PQS) and an iron chelator; 4-hydroxy-2-heptylquinoline (pseudan VII), which is an iron chelator, antibacterial compound and precursor of PQS; 4-hydroxy-2-nonylquinoline (pseudan IX) which is an iron chelator and antibacterial compound; 4-hydroxy-2-methylquinoline (pseudan I), and 4-hydroxy-2-nonylquinoline N-oxide.


* Corresponding author. Fax: +1 703 993 1046.
*E-mail address:* proyt@gmu.edu (P.W. Royt).

0045-2068/$ - see front matter © 2006 Elsevier Inc. All rights reserved.
doi:10.1016/j.bioorg.2006.10.004

*Keywords:* *Pseudomonas aeruginosa*; Periplasmic inclusion bodies; Iron; *Pseudomonas* quinolone signal; Pseudan; 4-Hydroxy-2-alkylquinoline; HAQ; PQS

## 1. Introduction

The Gram-negative bacterium *Pseudomonas aeruginosa* is an opportunistic pathogen that is capable of causing a variety of diseases in the immunocompromised host as well as chronic lung disease in the cystic fibrosis patient. The organism is known for secreting numerous virulence factors into its environment, as well as compounds collectively called 4-hydroxy-2-alkylquinolines (HAQs, Fig. 1). Two HAQs produced by *P. aeruginosa* are 4-hydroxy-2-heptylquinoline (pseudan VII) and 4-hydroxy-2-nonylquinoline

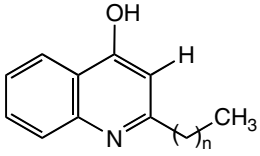


n = 0 4-hydroxy-2-methylquinoline (pseudan I)
n = 6 4-hydroxy-2-heptylquinoline (pseudan VII)
n = 8 4-hydroxy-2-nonylquinoline (pseudan IX)

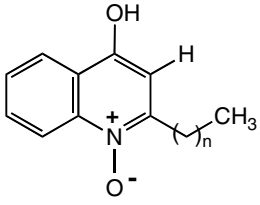


n = 6 4-hydroxy-2-heptylquinoline-N-oxide
n = 8 4-hydroxy-2-nonylquinoline-N-oxide

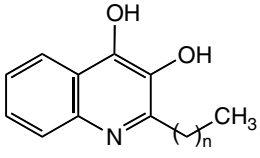


n = 6 3,4-dihydroxy-2-heptylquinoline
n = 8 3,4-dihydroxy-2-nonylquinoline

Fig. 1. Chemical structures of relevant HAQs.

(pseudan IX). Originally isolated in 1945, pseudan VII and IX were shown to have antibacterial activity [1]. More recently, it was shown that pseudan IX is an iron chelator [2,3]. Another HAQ, 3,4 dihydroxy-2-heptylquinoline, referred to as the *Pseudomonas* quinolone signal (PQS), is a quorum sensing molecule of this organism [4]. PQS, found in the lungs and sputum of patients with cystic fibrosis [5], controls expression of various virulence factors of the cell as it links to two other quorum sensing systems of this organism [6,7]. The iron-chelation property of the PQS has recently been reported [8]. As a direct precursor of the PQS, pseudan VII also plays a role in cell-to-cell signaling [9]. Members of another group of HAQs have an *N*-oxide group in place of the quinoline nitrogen, and a C7 or a C9 alkyl chain [10]. The C7 *N*-oxide was shown to have antistaphylococcal activity [11].

Inclusion bodies of prokaryotic cells serve various functions [12]. Some inclusion bodies are storage sites for carbon sources, such as those that contain lipid, glycogen, or starch. Other inclusion bodies store sulfur to be used as an energy source, whereas others store inorganic phosphate to be used in the synthesis of ATP. Some inclusion bodies carry out more specialized functions in the cell. Carboxysomes, for example, contain ribulose 1,5-diphosphate carboxylase needed for carbon dioxide fixation during photosynthesis [13]. Gas vacuoles keep aquatic bacteria buoyant, whereas magnetosomes, inclusions of iron oxide, serve to orient cells along a magnetic field [14]. Characteristic of prokaryotic inclusion bodies is the absence of a unit membrane defining them. These structures may instead be enclosed by a nonunit lipid membrane or by protein, or may have no surrounding membrane. Some inclusion bodies are located in the cytoplasm of the cell, whereas others are found in the periplasmic space.

The objective of this work was to determine the source of particulate matter apparently released from iron-rich *P. aeruginosa*. Transmission electron microscopy of these cells showed the presence of periplasmic inclusion bodies. Subsequent chemical characterization of the inclusion bodies revealed the presence of iron and five HAQs, one of which is the PQS.

## 2. Materials and methods

### 2.1. Bacterial strains and growth conditions

*Pseudomonas aeruginosa* ATCC strain 15692 (PAO1) was used in all experiments. It was maintained at −70 °C in Luria–Bertani broth containing 25% glycerol. Cells were grown in trypticase soy broth (TSB: DIFCO Laboratories), shaking at 100 rpm at 30 °C in a New Brunswick rotatory shaker. Typically, cultures were inoculated with logarithmic phase cells to an initial optical density of 0.02–0.04. Early logarithmic phase cells (5 h) and mid-logarithmic phase cells (24 h) were collected by centrifugation at 11,950*g* for 10 min at 4 °C.

### 2.2. Collection of extracellular inclusion bodies

Cultures were centrifuged at 2987*g* for 10 min at 4 °C. The spent media was filtered through a 0.45 μm filter, and the filtrate centrifuged at 265,000*g* (Ti70 rotor, Beckman Coulter Instruments) for 2 h at 4 °C. The resultant pellet was washed one time with 60 mM 3-(4-morpholino) propane sulfonic acid buffer (MOPS buffer), pH 7.2.

### 2.3. Fractionation of the inclusion bodies by TLC

Isolated inclusion bodies were treated with acidified ethyl acetate, following the procedure used by others to isolate the PQS from spent media of *P. aeruginosa* [15], and with *P. aeruginosa* rhamnolipids obtained from Jeneil Biosurfactant Co, Saukville, WI. Solubilization of the inclusion bodies occurred upon vortexing for 30 min. Samples were spotted on silica gel TLC plates that had been soaked in 5% w/v $KH_2PO_4$ and activated for 1 h at 100 °C. Separation of compounds occurred using methylene chloride:acetonitrile:dioxane, 17:2:1 [4].

### 2.4. Iron determination

A pellet of inclusion bodies was acid hydrolyzed with nitric acid/perchloric acid (1/1: v/v). Following dilution in 0.1 M Tris–HCl buffer, pH 7.8, iron was determined on a Perkin-Elmer 5001 PC Atomic Absorption Spectrophotometer (AAS).

### 2.5. Electron microscopy

(i) Transmission electron microscopy (TEM) was performed on pellets of 5 and 24 h cells, and on isolated inclusion bodies. Samples were resuspended in 4% formaldehyde/1% glutaraldehyde overnight at 4 °C, post-fixed in 1% osmium tetroxide, dehydrated in graded alcohols and embedded in Epon 812. Thin (50–90 nm) sections were stained with lead citrate and uranyl acetate and examined in a LEO912 electron microscope (Carl Zeiss SMT, Thornwood, NY). (ii) Scanning electron microscopy (SEM) was done on 24 h cells using a JEOL JSM-840 electron microscope with a $LaB_6$ electron emitter. The SEM was equipped with an energy dispersive X-ray analyzer (EDAX) using a Si(Li) crystal (Princeton Gamma-Tech, Princeton, NJ). The sample was fixed in 1% glutaraldehyde for 2 h, and dehydrated with acetone.

### 2.6. High resolution electrospray ionization mass spectrometry (ESI MS)

Electrospray ionization mass spectra were obtained on a Waters LCT Premier Time-Of-Flight (TOF) Mass Spectrometer. The instrument was operated in positive ion mode at a resolution of 10,000. The electrospray capillary voltage was 3 kV and the sample cone voltage was 60 V. The desolvation temperature was 225 °C and the desolvation gas was nitrogen at 300 L/h. Accurate masses were obtained using the lock spray mode with Leu-Enkephalin as the external reference compound. The ESI mass spectra were obtained via the direct loop injection method.

### 2.7. Gas chromatography–mass spectrometry (GC–MS)

GC–MS was performed on a Hewlett Packard 5890 Series II GC with a Hewlett Packard 5989 A Mass Spectrometer. The GC column was a Varian Factor Four Capillary Column Model VF-5 ms, with 30 m length, 0.25 mm interior diameter, and 0.25 μm film thickness. The mass spectrometer electron impact voltage was 70 eV.

### 2.8. Electron paramagnetic resonance spectroscopy (EPR)

EPR spectra were obtained using a conventional Bruker EMX 9.5 GHz spectrometer operating at room temperature with the sample nominally in the dark, although no attempt was made to exclude room light. Typical operating microwave power was 1 mW.

### 2.9. Nuclear magnetic resonance spectroscopy (NMR)

NMR spectra ($^1$H) were obtained on a Bruker DPX 300 spectrometer at room temperature in the solvents chloroform-*d*, dimethyl sulfoxide-$d_6$, or a solution of these two, and were referenced to internal tetramethylsilane ($\delta = 0$ ppm), or to known solvent or compound peaks.

## 3. Results

### 3.1. Extracellular aggregates in pellets of mid-logarithmic phase cells

A pellet of early logarithmic phase *P. aeruginosa* cells grown in the presence of high iron is pink, as seen in Fig. 2A. Earlier work reviewed that it is the cytoplasmic membrane of the cells that is pink in color [2]. After ethanol extraction of these membranes, the membranes were pale in color, and the extract pink [2]. Extracted from the membranes were pseudan VII and pseudan IX, both complexed to iron [3]. Pellets of mid-logarithmic phase cells are also pink, but have on top dark-colored aggregates (Fig. 2B). It became apparent that the aggregates were extracellular. Since the aggregates are visible to the naked eye, it was obvious that the aggregates were larger than the cells themselves, and hence not filterable through a 0.45 μm filter. It was demonstrated, however, that smaller particulate matter was filterable from the spent media of these cells. Ultracentrifugation of filtered spent media resulted in a dark brown pellet (Fig. 2C). Atomic absorption spectroscopy of these pellets revealed the presence of iron.

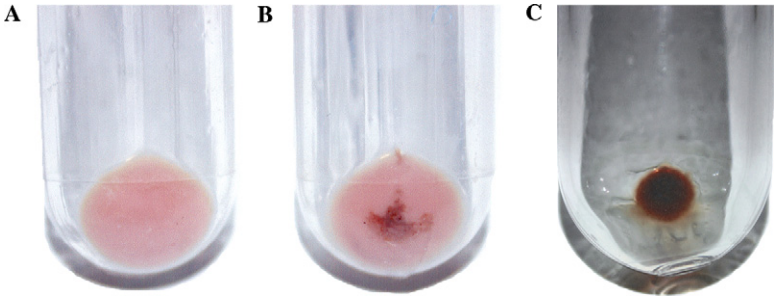


Fig. 2. Pellets of cells and aggregated particles. (A) Pellet of early logarithmic phase, iron-rich *P. aeruginosa* cells. (B) Pellet of mid-logarithmic phase, iron-rich cells containing aggregated particles. (C) Pellet resulting from the ultracentrifugation (265,000*g*/2 h) of filtered spent media of a mid-logarithmic phase culture.

### 3.2. TEMs of whole cells and isolated inclusion bodies

TEMs of the early and mid-logarithmic phase cells were taken to determine the source of the aggregated, iron-containing particles. The aggregates may consist of outer membrane vesicles or instead may be released inclusion bodies. TEMs of the early logarithmic phase culture did not show any unusual cell structures. However, the TEMs of the mid-logarithmic phase culture showed prominent dark inclusion bodies in ≈10% of the cells. Individual cells containing inclusion bodies are shown in Fig. 3. Fig. 3A shows a cell with multiple inclusion bodies, some of which are inside vacuoles, and a cell with one visible inclusion body. Fig. 3B through E each show a cell containing one large inclusion body of range 53–100 nm in diameter. Each inclusion body in Fig. 3B through E is within a vacuole within a cell. Fig. 3B reveals that a cell may have more than one

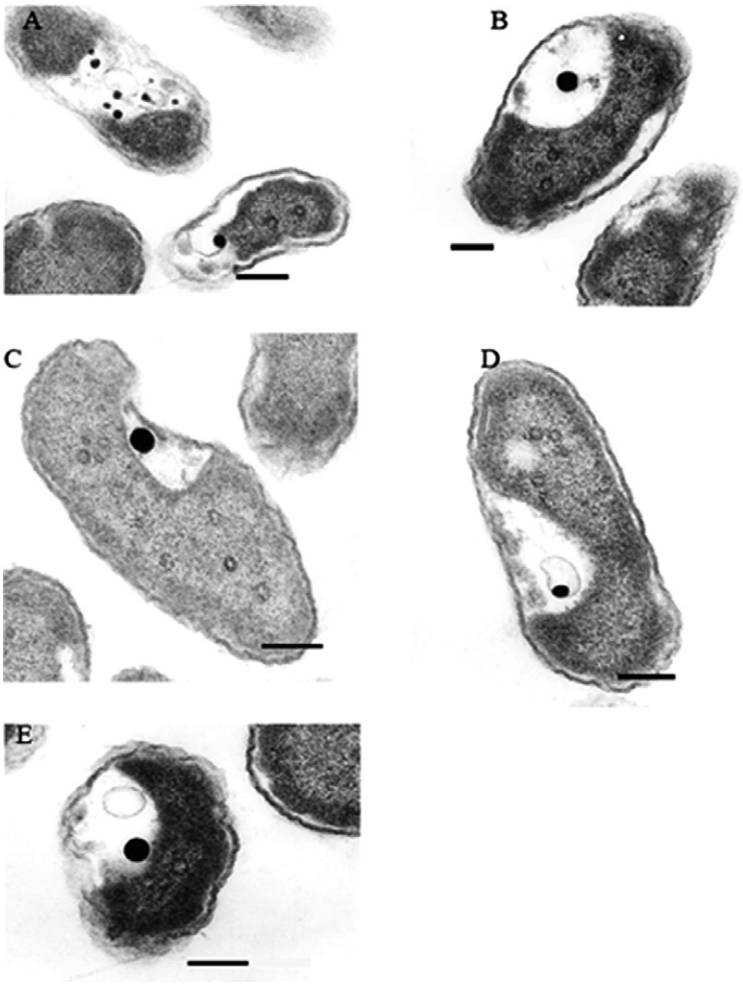


Fig. 3. TEMs of mid-logarithmic phase *P. aeruginosa*. Multiple inclusion bodies are seen in one cell in (A). Single inclusion bodies are seen in cells in (B) through (E). Bars = 200 nm.

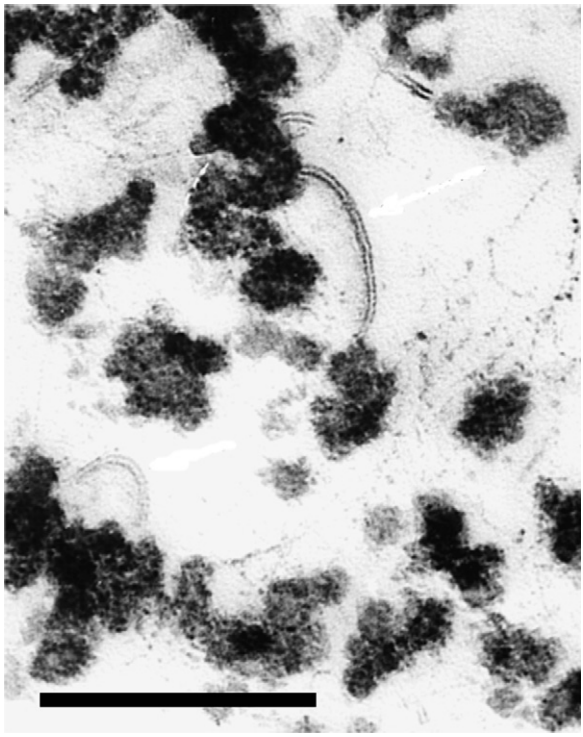

Fig. 4. TEM of the pellet seen in Fig. 2C. Bar = 200 nm.

vacuole. Fig. 3B and C show that these vacuoles are within the periplasm of the cells. In Fig. 3D, the inclusion body is seen within a smaller vacuole that is shown inside a larger vacuole: in Fig. 3E, the vacuole that the inclusion body is in appears to contain a smaller vacuole. No outer membrane vesicles are seen being shed from the cells, or detached from the cells in these TEMs. Also, no membrane is seen surrounding these intracellular inclusion bodies.

An electron micrograph of the pellet seen in Fig. 2C, the pellet of the aggregated particles collected by ultracentrifugation, reveals dark aggregates, the individual components of which range from 25 to 50 nm in diameter (Fig. 4). This TEM also shows the presence of a double layered structure.

### 3.3. SEM-EDAX of whole cells

To verify that the inclusion bodies seen inside the cells are indeed iron-containing and hence are the iron-containing pelleted aggregates isolated from the cells, an elemental analysis of intracellular inclusion bodies was compared with that of cells lacking inclusion bodies. Fig. 5A shows the back-scattered electron image of mid-logarithmic phase cells, one of which contains a bright area. The elemental analysis of a whole cell itself shows large amounts of carbon and phosphate, and modest amounts of other elements (Fig. 5B). The elemental analysis of the bright area reveals a high concentration of iron in addition to the elements found in the cell itself (Fig. 5C). The two iron peaks identify

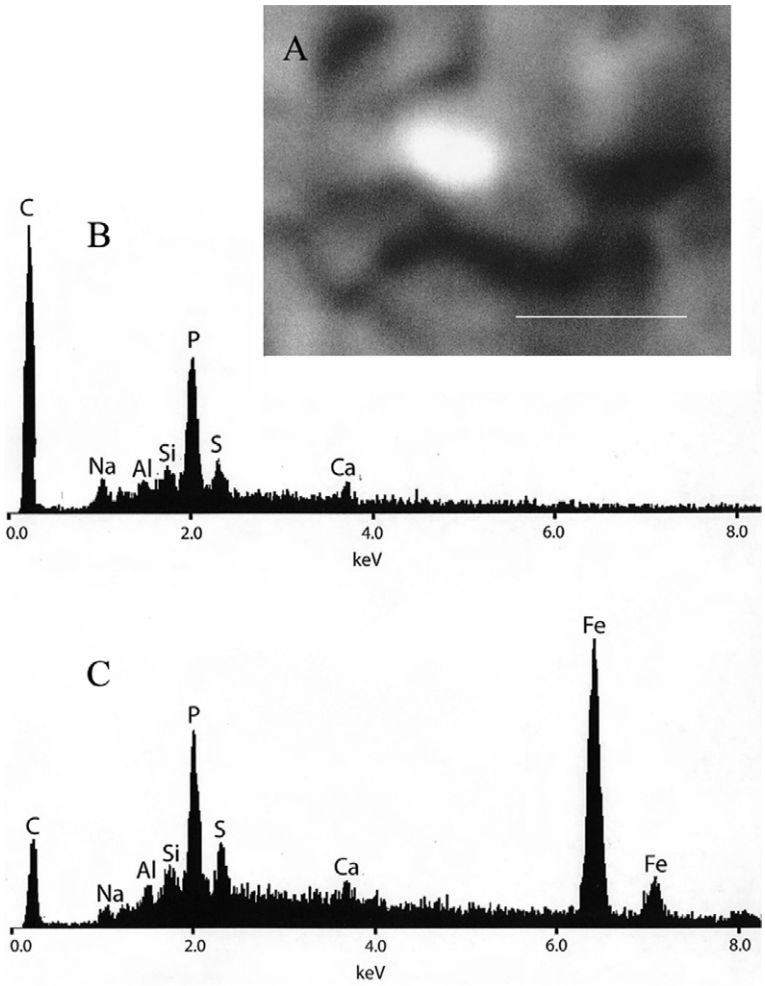


Fig. 5. SEM-EDAX of *P. aeruginosa*. (A) SEM back-scattered electron image of mid-logarithmic phase *P. aeruginosa*. Bar = 1 μm. (B) Elemental analysis of whole cells. (C) Elemental analysis of the bright spot.

the types of X-rays produced: the higher energy peak is a K-β peak in that it represents the X-rays emitted by M-shell electrons going to the K-shell, and the lower energy peak is a K-α peak representing X-rays emitted from electrons going from the L-shell to the K-shell.

### *3.4. The chemical composition of the inclusion bodies in the pellet of 24 h-old cells as revealed by TLC, ESI–MS, GC–MS, NMR, AAS, and EPR*

Pelleted inclusion bodies were extracted with rhamnolipid and with acidified ethyl acetate. Thin layer chromatograms of these extracts revealed the appearance of at least four bands (data not shown), one of which, $R_f = 0.55$, was fluorescent blue.

ES–MS of whole inclusion bodies (Fig. 6) showed a peak of *m/z* 272.2010 consistent with the $C_{18}H_{26}NO$ formula, or pseudan IX (Fig. 1). A peak was also observed at *m/z*

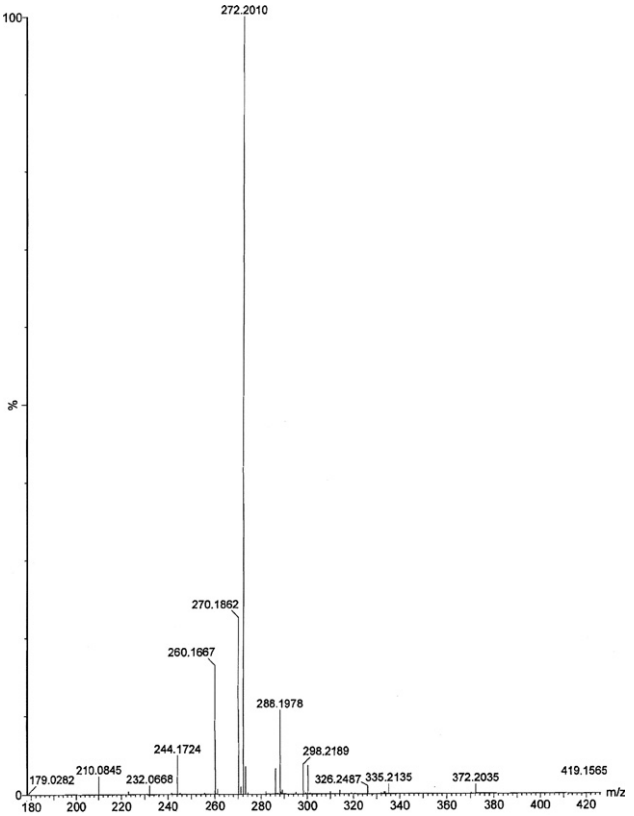


Fig. 6. The high resolution electrospray mass spectrum of whole inclusion bodies.

288.1978 ($C_{18}H_{26}NO_2$) which may be 4-hydroxy-2-nonylquinoline-*N*-oxide, with establishment of structure via ease of loss of the oxygen atom on the nitrogen [16]. The peak of *m*/*z* 270.1862 ($C_{18}H_{24}NO$ formula) is of dehydrated, 4-hydroxy-2-nonylquinoline-*N*-oxide, and a peak at *m*/*z* 244.1724 ($C_{16}H_{22}NO$) is pseudan VII, and finally, a peak at 260.1667 ($C_{16}H_{22}NO_2$ formula) is 3,4-dihydroxy-2-heptylquinoline. Absent from the spectra is dehydrated, 4-hydroxy-2-heptylquinoline-*N*-oxide which would have a molecular weight of 242. This absence suggests that the position of the second oxygen atom in the two compounds, i.e., the C7 compound and the C9 compound differs, in that one is a protonated *N*-oxide, as in the C9 compound, and the other a hydroxyl group. Hence, the peak at 260.1667 is that of 3,4-dihydroxy-2-heptylquinoline.

GC–MS was also carried out using the whole inclusion bodies, and using the blue fluorescent spot eluted from the thin layer chromatogram. The total ion chromatogram (TIC) of the whole inclusion bodies revealed about 20 major peaks. Pseudan VII was identified at 23.54 min, and pseudan IX was identified at 23.90, 24.02, and 25.20 min. 4-Hydroxy-2-nonylquinoline-*N*-oxide and dehydrated 4-hydroxy-2-nonylquinoline-*N*-oxide were also evident. The TIC did not reveal the presence of 3,4-dihydroxy-2-heptylquinoline, but did show the presence of dehydrated 3,4-dihydroxy-2-heptylquinoline. Also present in the TIC at 23.54 min as well as in other peaks is 4-hydroxy-2-methylquinoline, or pseudan

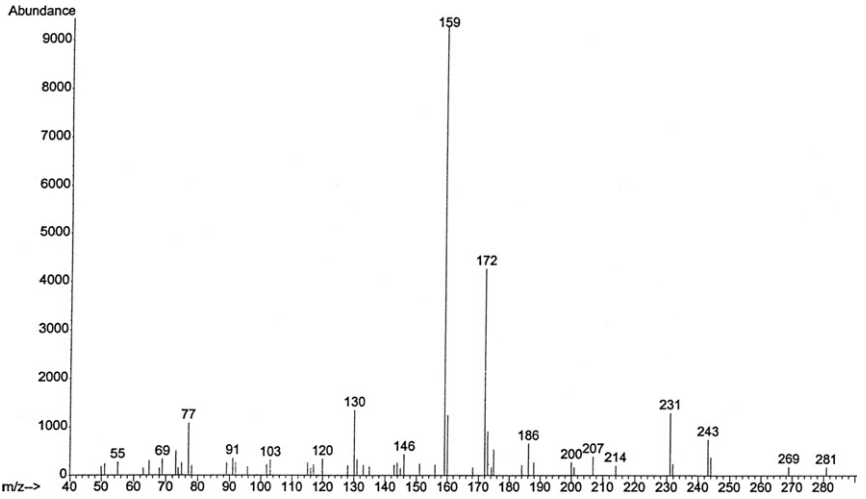


Fig. 7. Electron impact mass spectrum of the 23.54 min peak of the GC–MS of whole inclusion bodies. The sample was dissolved in methanol.

I. Fig. 7 is the mass spectrum of the 23.54 min peak showing an *m*/*z* 159 peak that is both the molecular weight of pseudan I and a mass spectrally-produced pseudan VII and IX fragment. The presence of pseudan I outside the mass spectrometer is unambiguously supported by NMR data. The TIC of the whole inclusion bodies also revealed *m*/*z* 56 in several peaks, which may be iron or an organic fragment. The TIC of the blue fluorescent spot eluted from the thin layer chromatogram and dissolved in methylene chloride exhibited one major peak and about 10 minor peaks. The mass spectrum of the most intense peak at 15.26 min revealed a C9 compound. A peak at 18.59 min is less intense, but has a mass spectrum similar to that of the 15.26 peak, and additionally has a fragment of *m*/*z* 241 that corresponds to dehydrated 3,4-dihydroxy-2-heptylquinoline. The TIC of the eluted blue fluorescent spot dissolved in methanol contained peaks of 15.26 and 18.59 min as above. The mass spectrum of the intense 15.26 peak was identical to that of the 15.26 peak above. The mass spectrum of the 18.59 peak showed a peak at *m*/*z* 159, the molecular weight of pseudan I. Peaks at 23.17 and 29.63 min revealed the presence of a *m*/*z* peak of 269, which may be dehydrated, 4-hydroxy-2-nonylquinoline-*N*-oxide.

A $^{1}$H NMR spectrum of whole inclusion bodies reconfirms the presence of pseudan I, pseudan VII, and pseudan IX. The pseudan I assignments are: $\delta$ 2.34 (s, 3 H, $CH_3$ of **1**), 6.01 (s, 1 H, $H^3$ of **1**), 7.21 (t, $J = 7$ Hz, 1 H, $H^{6\text{ or }7}$ of **1**), 7.48 (m, 1 H, $H^8$ of **1**), 7.53 (m, 1 H, $H^{6\text{ or }7}$ of **1**), 8.16 (d, $J = 8$ Hz, 1 H, $H^5$ of **1**), 11.35 (br s, 1 H, OH of **1**). The pseudan VII and pseudan IX assignments in the spectrum are: $\delta$ 0.85 (t, $J = 6$ Hz, 3 H, $CH_3$ of **2** and **3**), 1.28 (m, 10 H, $H^{11-14}$ of **2** and $H^{11-16}$ of **3**), 1.67 (m, 2 H, $H^{10}$ of **2** and **3**), 2.56 (t, $J = 8$ Hz, 2 H, $H^9$ of **2** and **3**), 6.03 (s, 1 H, $H^3$ of **2** and **3**), 7.21 (t, $J = 7$ Hz, 1 H, $H^{6\text{ or }7}$ of **2** and **3**), 7.48 (m, 1 H, $H^8$ of **2** and **3**), 7.53 (m, 1 H, $H^{6\text{ or }7}$ of **2** and **3**), 8.16 (d, $J = 8$ Hz, 1 H, $H^5$ of **2** and **3**), 11.21 (br s, 1 H, OH of **2** and **3**) (Fig. 8). These assignments were made by comparison with literature values for synthetic compounds and spectra done in our laboratory on synthetic compounds [17,18].

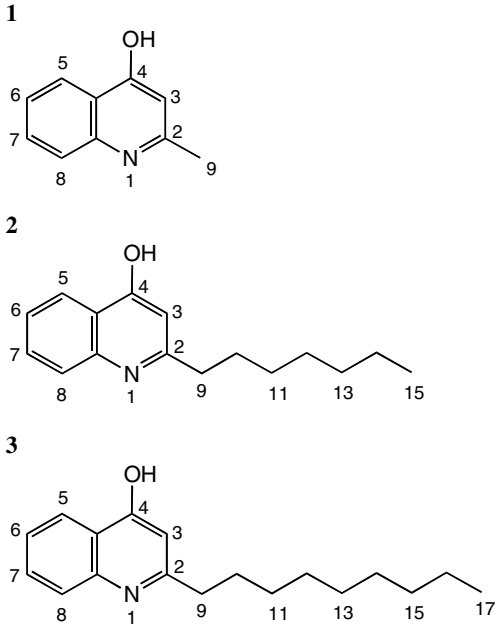


Fig. 8. Numbering scheme for the $^{1}$H NMR spectra of (1) a methyl quinoline, (2) a heptyl quinoline, and (3) a nonyl quinoline.

The NMR spectrum exhibits pseudan I, pseudan VII, and pseudan IX in relative mole-based amounts of 1.00, 0.99, and 1.10. A second $^{1}$H NMR spectrum was taken of the blue fluorescent spot eluted from the thin layer plate. The spectrum showed broad and sharp peaks indicative of two or more chemical species exchanging at an intermediate rate as might occur if ligands were being attached and detached from $Fe^{3+}$, or alternatively, a paramagnetic metal ion attached to and broadening organic ligands. Absence of a peak in the 11 ppm OH region means the absence of hydroxyls: any hydroxyl present, though, may have been deprotonated.

AAS of the inclusion bodies revealed the presence of iron, as did EPR that was carried out to determine the oxidation state of the iron. The signal is centered at $g = 4.2$ and has a width of 215 G. This is consistent with the $M_S = 3/2$ doublet of $Fe^{3+}$ in a low symmetry environment which would ideally give $g = 30/7$ (4.3). The line is reasonably symmetric, unlike that expected for a powder pattern. This may suggest that the spin is somewhat delocalized and that the width is due to unresolved hyperfine interactions with surrounding hydrogen atoms. The $g = 4.2$ value puts the *Pseudomonas* compound in the same range as ferrichrome and ferrichrome A from *Ustilago sphaerogena*, and $FeCl_3$ in excess aqueous sodium citrate [19]. The EPR work was not done in solution, and as a result the environment around the $Fe^{3+}$ is not likely to be changed by solvent substitution.

## 4. Discussion

The purpose of this research was to determine the source of the aggregated particles on pellets of mid-logarithmic phase, iron-rich *P. aeruginosa*. Electron microscopy of

mid-logarithmic phase cells revealed dark inclusion bodies in vacuoles of the cells, inclusion bodies absent in the early logarithmic phase cells. Further examination of the TEMs revealed that the inclusion bodies were in the periplasm of the cells. The TEMs did not reveal blebs on the outside of the cells, indicating that under these conditions of growth the cells were not producing outer membrane vesicles as reported by others to occur in *P. aeruginosa* [20–23].

Ultracentrifugation of spent media of mid-logarithmic phase cells resulted in a dark pellet that contains iron. The TEM of this pellet showed dark aggregates that are not surrounded by a unit membrane or a nonunit membrane, telling us once again that the aggregates do not consist of membrane vesicles.

Are the inclusion bodies seen inside the cell the aggregated particles collected by ultracentrifugation? The elemental analysis of the back-scattered image of mid-logarithmic phase cells produced by SEM-EDAX shows a dense iron-containing area below the surface of the cell (Fig. 5). This leads us to conclude that the iron-containing aggregates pelleted from the filtered, spent media of cells consist of the cellular inclusion bodies. It is apparent from these studies that the inclusion bodies are released from the cell, and enter the environment of the cell. At this time, it is not known if the aggregates of inclusion bodies we see on the pelleted cells (Fig. 2B) are caused by the centrifugation of the cells, or if aggregation occurs naturally in the medium.

Our attention turned to the chemical analysis of the inclusion bodies. We have shown by NMR and GC–MS that the whole inclusion bodies contain pseudan VII and IX. Pseudan I, $m/z$ of 159, appears multiple times in the GC mass spectra. It is possible that it is a fragment formed in the mass spectrometer as occurs in synthetic samples of pseudan VII and IX [17]. However, in the NMR, fragmentation does not occur, and hence, pseudan I is a constituent of the inclusion bodies. Others have previously identified pseudan I in *P. aeruginosa* [16]. The 1:1:1 stoichiometry of pseudan I, VII, and IX is suggesting the complexation ratio of chelators to iron. The ES–MS also shows the presence of pseudan VII and IX. GC–MS of the whole inclusion bodies indicates dehydrated 3,4-dihydroxy-2-heptylquinoline, and ES–MS shows the parent 3,4-dihydroxy-2-heptylquinoline. GC–MS and ES–MS of the whole inclusion bodies show dehydrated 4-hydroxy-2-nonylquinoline-*N*-oxide, and GC–MS shows 4-hydroxy-2-nonylquinoline-*N*-oxide itself. The eluted blue fluorescent spot on the thin layer plate contains the two dehydrated compounds discussed in this paragraph. From these analyzes, we conclude that the inclusion bodies contain oxidized iron, pseudan I, pseudan VII, pseudan IX, 4-hydroxy-2-nonylquinoline-*N*-oxide, and 3,4-dihydroxy-2-heptylquinoline, the PQS. The dehydrated compounds detected are produced in the instruments.

To enter another cell the PQS and its precursor must be released from the inclusion bodies. Others have shown that rhamnolipid, a surfactant produced by *P. aeruginosa* late in growth [24] stimulates the uptake of hydrophobic compounds by this organism [25], and that the bioactivity of the PQS is increased by rhamnolipid [26]. Work in our laboratory has shown that rhamnolipid does indeed solubilize the inclusion bodies as indicated by TLC. We suggest that cell-surface solubilization of the inclusion bodies occurs via the rhamnolipids. Such solubilization would serve to release the packaged PQS and its precursor, as well as pseudan VII and IX to be used as antimicrobial compounds. Solubilization of the inclusion bodies would also recycle ion.

It has recently been reported that *P. aeruginosa* strain PA14 packages the PQS as well as pseudan VII and pseudan IX into outer membrane vesicles [23]. Differences in growth

conditions, e.g., media components, aeration, and temperature of growth as well as cell strain, may account for the apparent discrepancy between those findings and our results reported here. In our study, the TEMs of a culture producing inclusion bodies did not show the presence of outer membrane vesicles on the cells (Fig. 3), nor did the TEM of the inclusion bodies show membranes around the inclusion bodies (Fig. 4).

At this time, the method of formation of the inclusion bodies and the role that any membranes may play in such formation are not known. The finding of multiple small inclusion bodies in cells (Fig. 3A) may suggest that the larger inclusion bodies result from the coalescing of the smaller bodies. It is seen that one cell may have more than one periplasmic vacuole (Fig. 3B). The smaller vacuoles found within the larger vacuoles (Fig. 3D and E) may be cross sections of vacuoles on the opposite side of the cell invaginated in. However, close examination of these vacuoles does not reveal a membrane with a bilayer structure, and hence, at this time the origin and composition of these membranous-like structures are not known. It is also noted that inside the periplasmic vacuoles the inclusion bodies are larger, 53–100 nm, than are the pelleted inclusion bodies of 25–50 nm in diameter. Also, the pelleted inclusion bodies are irregular in shape, unlike the rounded, intracellular inclusion bodies. Solubilization of the inclusion bodies, as discussed above, may be occurring during the procedure used to collect the extracellular inclusion bodies. We also note the ring-shaped structures in the cytoplasm of cells in Fig. 3, and question the role of these structures in overall cell physiology.

We are currently investigating the method of release of the inclusion body from the cell. The large size of the inclusion bodies precludes the use of outer membrane components of drug efflux pumps used to release small drugs from Gram-negative bacteria [27]. The double-layered structures in the TEM of the pelleted inclusions bodies (Fig. 4) may be membrane fragments, suggesting that the inclusion bodies are released from the cells upon breaking the outer membrane. If that is the case, the periplasmic location of the inclusion bodies provides the cell with a means to release the HAQs and iron without killing the cell.

## 5. Conclusion

Growing in a high iron-containing environment, *P. aeruginosa* produces periplasmic inclusion bodies that contain oxidized iron and five HAQs: 3,4-dihydroxy-2-heptylquinoline which is the *Pseudomonas* quinolone signaling compound and iron chelator; 4-hydroxy-2-heptylquinoline (pseudan VII), which is an iron chelator, antibacterial compound and precursor of PQS; 4-hydroxy-2-nonylquinoline (pseudan IX) which is an iron chelator and antibacterial compound; 4-hydroxy-2-methylquinoline (pseudan I), and 4-hydroxy-2-nonylquinoline *N*-oxide. These inclusion bodies are unique to prokaryotic cells. They are not depots of a carbon or energy source, but rather contain compounds known to have specialized functions: by containing iron, the inclusion bodies are iron depots; by containing antimicrobial compounds, the inclusion bodies may ward off competitors within the environment of the cell; and by containing a signaling compound as well as its precursor, the inclusion bodies may contribute to population synchrony and virulence.

## References

[1] E.E. Hays, I.C. Wells, P.A. Katzman, C.K. Cain, A. Jacobs, S.A. Thayer, E.A. Doisy, W.L. Gaby, E.C. Roberts, R.D. Muir, C.J. Carroll, L.R. Jones, N.J. Wade, J. Biol. Chem. 159 (1945) 725–750.

[2] P.W. Royt, Biochim. Biophys. Acta 939 (1988) 493–502.
[3] P.W. Royt, R.V. Honeychuck, V. Ravich, P. Ponnaluri, L.K. Pannell, J.S. Buyer, V. Chandhoke, W.M. Stalick, L.C. DeSesso, S. Donohue, R. Ghei, J.D. Relyea, R. Ruiz, Bioorg. Chem. 29 (2001) 387–397.
[4] E.C. Pesci, J.B. Milbank, J.P. Pearson, S. McKnight, A.S. Kende, E.P. Greenberg, B.H. Iglewski, Proc. Natl. Acad. Sci. USA 96 (1999) 11229–11234.
[5] D.N. Collier, L. Anderson, S.L. McKnight, T.L. Noah, M. Knowles, R. Boucher, U. Schwab, P. Gillian, E.C. Pesci, FEMS Microbiol. Lett. 215 (2002) 41–46.
[6] S.L. McKnight, B.H. Iglewski, E.C. Pesci, J. Bacteriol. 182 (2000) 2702–2708.
[7] S.P. Diggle, K. Winzer, S.R. Chhabra, K.E. Worrall, M. Camara, P. Williams, Mol. Microbiol. 50 (2003) 29–43.
[8] F. Bredenbruch, R. Geffers, M. Nimtz, J. Buer, S. Häussler, Environ. Microbiol. 8 (2006) 1318–1329.
[9] E. Déziel, F. Lépine, S. Milot, J. He, M.N. Mindrinos, R.G. Tompkins, L.G. Rahme, Proc. Natl. Acad. Sci. USA 101 (2004) 1339–1344.
[10] J.W. Cornforth, A.T. James, Biochem. J. 63 (1956) 124–130.
[11] Z.A. Machan, G.W. Taylor, T.L. Pitt, P.J. Cole, R. Wilson, J. Antimicrob. Chemother. 30 (1992) 615–623.
[12] J.M. Shively, Ann. Rev. Microbiol. 28 (1974) 167–187.
[13] J.M. Shively, F. Ball, D.H. Brown, R.E. Saunders, Science 182 (1973) 584–586.
[14] R. Blakemore, Science 190 (1975) 377–379.
[15] S. McGrath, D.S. Wade, E.C. Pesci, FEMS Microbiol. Lett. 230 (2004) 27–34.
[16] G.W. Taylor, Z.A. Machan, S. Mehmet, P.J. Cole, R. Wilson, J. Chromatogr. B 664 (1995) 458–462.
[17] R.R. Pant, Ph.D. Dissertation, George Mason University, 2006.
[18] R. Somanathan, K.M. Smith, J. Heterocyclic Chem. 18 (1981) 1077–1079.
[19] D.J. Ecker, J.R. Lancaster Jr., T. Emery, J. Biol. Chem. 257 (1982) 8623–8626.
[20] J.L. Kadurugamuwa, T.J. Beveridge, J. Bacteriol. 177 (1995) 3998–4008.
[21] J. L Kadurugamuwa, T.J. Beveridge, J. Bacteriol. 178 (1996) 2767–2774.
[22] M. Renelli, V. Matias, R.Y. Lo, T.J. Beveridge, Microbiology 150 (2004) 2161–2169.
[23] L.M. Mashburn, M. Whiteley, Nature 437 (2005) 422–425.
[24] F.G. Jarvis, M.J. Johnson, J. Am. Chem. Soc. 71 (1949) 4124–4126.
[25] W.H. Noordman, D.B. Janssen, Appl. Environ. Microbiol. 68 (2002) 4502–4508.
[26] M.W. Calfee, J.G. Shelton, J.A. McCubrey, E.C. Pesci, Infect. Immun. 73 (2005) 878–882.
[27] H. Nikaido, J. Bacteriol. 178 (1996) 5853–5859.